Tumor Biol. (2011) 32:301–310
DOI 10.1007/s13277-010-0122-9

RESEARCH ARTICLE

Suppression of bladder cancer growth in mice by adeno-associated virus vector-mediated endostatin expression

Jian Gang Pan · Xing Zhou · Ge Wa Zeng · Rui Fa Han

Received: 10 August 2010 / Accepted: 12 October 2010 / Published online: 30 October 2010

Abstract Novel treatment strategies such as gene therapy are warranted in view of the failure of current treatment approaches to cure a high percentage of patients with advanced bladder cancers. Testing of the hypothesis that blocking the angiogenic switch may keep tumour growth in check has been facilitated by the discovery of endogenous inhibitors of angiogenesis and has also added another research dimension to the field of cancer gene therapy. Consequently, the concept of targeting the tumour vasculature with anti-angiogenic agents has emerged as an attractive new strategy in the treatment of cancer. Targeted biological therapies that selectively interfere with tumour angiogenesis could improve survival among patients with bladder cancer. Endostatin is a tumour-derived angiogenesis inhibitor and is the first endogenous inhibitor of angiogenesis to be indentified in a matrix protein. Gene therapy represents an attractive approach to treat cancers and other chronic diseases. The development of an effective delivery system is absolutely critical to the usefulness and safety of gene therapy. At present, the adeno-associated virus (AAV) vector has the most promising potential in view of its non-pathogenicity, wide tropisms and long-term transgene expression in vivo. Gene therapy studies using different serotypes of recombinant AAV (rAAV) as delivery vehicles have proved rAAVs to be an effective modality of cancer gene therapy. In the present study, an IgG fragment was inserted at the start of the sequence coding for endostatin with the aim of enabling continuous secretion of endostatin the serum. We also investigated the suppression effect of AAV-mediated endostatin expression on endothelial cells and in mice xenograft models of bladder cancer. Our data demonstrates that rAAV-endostatin controlled tumour cell growth and achieves strong anti-tumour efficacy in vivo.

Keywords Bladder cancer · Gene therapy · Endostatin · Adeno-associated virus (AAV)

Introduction

Bladder cancer is a disease characterised by high tumour-recurrence rates despite therapy using resection, intravesical chemotherapy or immunotherapy with BCG. On the basis of clinical presentation, cytotoxic chemotherapy is delivered via intravesical instillation, in patients with localised disease, after surgical resection [1] or as systemic combination chemotherapy [2]. Whereas systemic chemotherapy is the mainstay of treatment for metastatic bladder cancer, it is limited by significant toxicity, low complete response rates ranging about 36% and long-term survival incidence of only 4% [2–4]. Novel treatment strategies such as gene therapy are warranted in view of the failure of current treatment approaches to cure a high percentage of patients with advanced bladder cancers [5].

Bladder cancer, classified as a solid tumour, depends on angiogenesis for sustained growth and blood-borne metastatic spread [6]. Testing of the hypothesis that blocking the angiogenic switch may keep tumour growth in check has been facilitated by the discovery of endogenous inhibitors

J. Pan and X. Zhou contributed equally to this paper.

J. G. Pan · X. Zhou (✉) · G. W. Zeng
The Second Affiliated Hospital of Guangzhou Medical University,
Changgang Dong Lu, No. 250,
Guangzhou 510260, China
e-mail: zhouxingboshi@163.com

R. F. Han
Tianjin Institute of Urology, The Second Hospital of Tianjin Medical University,
Tianjin 300300, China

of angiogenesis and has also added another research dimension to the field of cancer gene therapy [7]. Consequently, the concept of targeting the tumour vasculature with anti-angiogenic agents has emerged as an attractive new strategy in the treatment of cancer [8].

Targeted biological therapies that selectively interfere with tumour angiogenesis could improve survival among patients with bladder cancer. Endostatin is a tumour-derived angiogenesis inhibitor and is the first endogenous inhibitor of angiogenesis to be indentified in a matrix protein. Endostatin specifically inhibits the proliferation and migration of endothelial cells and induces their apoptosis without direct cytotoxic effects on tumour cells [9].

Most therapeutic investigations of endostatin have utilised its purified protein form. There are, however, several potential concerns with such a treatment strategy. First, the protein-purification process may denature endostatin and the resultant yield rates may be low. Second, as a proteinaceous drug, endostatin has a short half-life in vivo and this raises concerns regarding maintenance of therapeutically effective serum levels. Finally, the need to deliver angiogenic inhibitors such as endostatin on a chronic basis may lead to practical difficulties in clinical situations. One possible approach to overcoming some of these issues may be the utilisation of a gene therapy strategy [8].

Gene therapy represents an attractive approach to treat cancers and other chronic diseases. The development of an effective delivery system is absolutely critical to the usefulness and safety of gene therapy. At present, the adeno-associated virus (AAV) vector has the most promising potential in view of its non-pathogenicity, wide tropisms and long-term transgene expression in vivo [10]. Gene therapy studies using different serotypes of recombinant AAV (rAAV) as delivery vehicles have proved rAAVs to be an effective modality of cancer gene therapy [11–15].

AAVs are single-stranded DNA viruses that encode for two viral proteins, namely Rep and Cap. Genes coding for these two proteins are removed from the defective vectors used in gene therapy. Similar to adenoviruses, AAVs can infect both dividing and non-dividing cells. The DNA of AAVs, however, integrates into the host cell genome in a manner similar to the retroviruses. AAV vectors pose minimal toxicity since their wild-type version does not cause pathological effects in humans while they integrate specifically into chromosome 19 of the human genome [16]. Such specificity reduces the risks of insertional mutagenesis encountered in retroviral-mediated gene transfer. In addition, the site of integration does not encode for any important gene [17].

Based on a PubMed search (using the key terms: ‘endostatin’, ‘bladder cancer’ and ‘adeno-associated virus’), we ascertained that very little information is available regarding the effects of endostatin used in combination with AAVs in the treatment of bladder cancer. In the present study, an IgG fragment was inserted at the start of the sequence coding for endostatin with the aim of enabling the continuous secretion of endostatin the serum. We also investigated the suppression effect of AAV-mediated endostatin expression on the endothelial cells and in mice xenograft models of bladder cancer. Our data demonstrates that rAAV-endostatin controlled tumour cell growth and achieves strong anti-tumour efficacy in vivo. These findings provide a foundation for the development of potential targeted clinical therapies for bladder cancer in humans.

Materials and methods

Cell line and culture

The AAV-293 cell line was obtained from the Shanghai Institute for Sciences, Chinese Academy of Sciences (Shanghai, China). The HUVEC cell line (human umbilical vein endothelial cell) was obtained from the Tianjin Institute of Urology (Tianjin, China). Human bladder cancer cell line T24 was purchased from the Shanghai Cell Collection (Shanghai. China). The AAV-293 cells were cultured in Dulbecco’s modified minimum essential medium (DMEM) supplemented with 10% heat-inactivated foetal bovine serum (FBS). The T24 and HUVEC cells were grown in RPMI 1640 supplemented with 5% heat-inactivated FBS at 37°C in 5% CO_2.

rAAV construction and production

Human IgG-endostatin was amplified from plasmid pIRES-endostatin by polymerase chain reaction (PCR) using primers that included forward (5′-GACATCGATATGA AATG-CAGCTGGGTTATC) and reverse (3′-TATGGATCC CTACTTGGAGGCAGTCATG) sequences (94°C for 1 min, 57°C for 1 min, 72°C for 1 min). The IgG fragment was engineered to signal secretion. This fragment was then inserted into the plasmid pCMV-MCS to create pCMV-IgG-endostatin. This vector contains a transgene expression cassette that carries the human cytomegalovirus (CMV) promoter to catalyse transgene expression. Following this, the pCMV-IgG-endostatin and plasmid AAV (pAAV)-MCS complexes were digested by the enzyme *Not*I to determine the pAAV-IgG-endostatin complex to ensure stability of the sequences, given that the transgene expression cassette is flanked by the non-coding inverted terminal repeats (ITRs) that are the only wild-type viral sequences present in this recombinant vector genome and are essential for packaging of the viral vector DNA (Fig. 1). All the constructs were sequenced by electrophoresis, and the DNA sequence service of TAKARA Company was used to confirm the correct sequences.

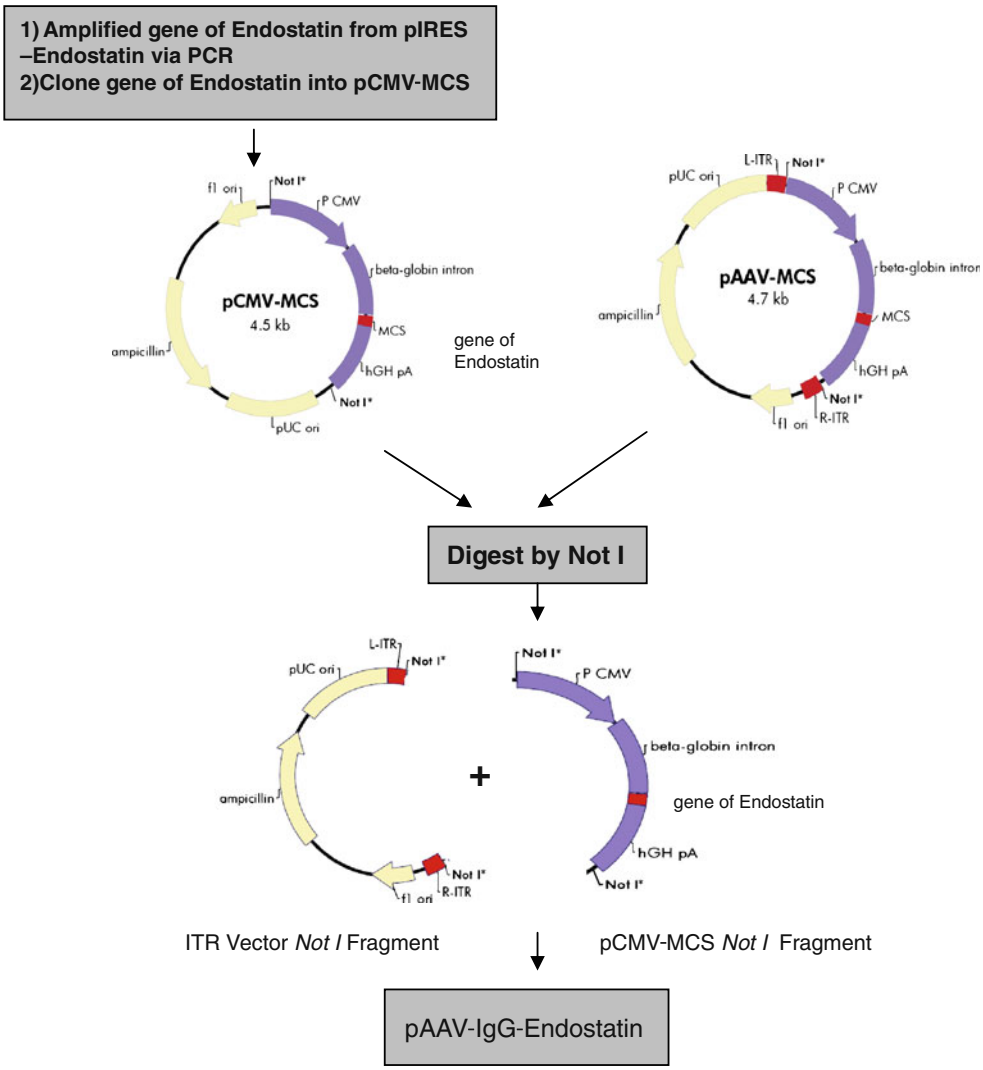

Fig. 1 Constructive step of pAAV-IgG-Endostatin. Human IgG-Endostatin (694 bp) fragment was amplified from plasmid pIRES-endostatin by PCR, and then inserted into plasmid pCMV-MCS to create pCMV-IgG-Endostatin. Then pCMV-IgG-endostatin and pAAV-MCS were digested by enzyme *Not*I to construct pAAV-IgG-endostatin

The rAAV vectors were produced by a three-plasmid transfection and purification method. Briefly, AAV-293 cells at 70–80% confluence were transfected with the rAAV, pAAV-RC and pHelper plasmids using the standard $CaCl_2$ technique for a period of 72 h. Cells were grown in DMEM that did not contain phenol and pyruvate and supplemented with 10% FBS. The medium was refreshed 2 h prior to transfection as well as on the day after transfection. Recombinant AAV was harvested 72 h after transfection by removing the medium and adding lysis buffer, then pooled and incubated for 1 h with DNAse—that is, after harvesting the cells, three freeze/thaw cycles were carried out and the sample was treated with DNAse [18]. After centrifugation, the rAAV was purified using a three-step procedure, which involves chloroform treatment, PEG/NaCl precipitation and chloroform extraction [19]. The viral stock was then concentrated to the required volume and stored at −80°C until further use.

Characterisation of the rAAV stocks included AVSachTM ELISA (**V**ector Gene Technology Company Limited, Beijing, China) assay for viral titre, SDS-PAGE analysis for visualisation and confirmation of the presence of only the specified three capsid proteins, as well as electronic microscopy for visualising its shape.

Transduction assay of reporter gene in vitro

T24 cells were grown to ~80% confluence, trypsinised and then counted. An aliquot containing 10^4 cells was then suspended in a serum and antibiotic-free medium. Next, rAAV vectors containing the EGFP (rAAV-EGFP; **V**ector Gene Technology Company) cassettes were added at a gradient titre of 10^3, 10^4, 10^5, 10^6 and 2×10^6 virus particle (vp) and then incubated at 37°C for 1 h. The medium was then removed and the plates were washed three times with DMEM. Fresh DMEM medium containing 10% was then added. After infection for about 72 h, EGFP expression was detected by fluorescence microscope with a digital camera apparatus and analysed by flow cytometry to determine the appropriate titre value to be applied in later steps of the study.

Cell stability after rAAV transduction

T24 cells were plated at a density of 10^5 cells in plates and infected with pAAV-IgG-endostatin at a dosage of 10^6 vp; 72 h later: (a) cells were harvested by trypsinisation followed by washing with PBS and then fixed in 70% ethanol overnight. Prior to analysis by FACS, the cells were treated with 1 mg/ml RNase for 30 min. The samples were then washed with PBS twice and resuspended in 25 mg/ml propidium iodine (PI) in PBS at a concentration of 1×10^6 cells/ml. These cells were stained with PI in the dark for 15 min and analysed by FACS to evaluate cell cycle distribution. (b) Genomic DNA was extracted from the cells infected with the rAAV-IgG-endostatin complex. The DNA sequence of endostatin was identified by PCR and sequence analysis to detect the infection efficiency.

Endostatin enzyme immunoassay

Cells were plated in vitro (1×10^6 per well in 6-well dishes) with 2 ml of appropriate growth medium and incubated for 24 h. Blood samples from the mice were collected in vivo by cardiac puncture, and the serum was separated by centrifugation. In both cases, a 100-μl sample was analysed using the Endostatin ELISA Kit (RayBiotech, Inc., Norcross, GA).

Cell-viability assay

HUVEC cells were plated in 96-well dishes at 1×10^4 cells per well. Eighteen hours later, the cells were infected with rAAV-IgG-endostatin at a dose of 1×10^6 vp for at least 6 h in a serum-free and antibiotic-free medium, which was followed by incubation in the complete medium for 24, 48 and 72 h, respectively. The cells without infection were used as negative control and infection of rAAV-EGFP as positive control. Cell viability was evaluated by assay with 3-(4,5-dimethylthiazol-2-yl)-2, 5-diphenyl tetrazolium bromide (MTT) every 24 h after infection. Briefly, 20 μl of MTT solution was added into each well containing 100 μl of PBS. After incubation at 37°C for 4 h, the MTT solution in the well was gently removed and 100 μl of DMSO was added. Cell viability was calculated based on the following formula:

$$\text{Cell viability}(\%) = \left[\text{OD570 of } \frac{\text{experimental}}{\text{control}}\right] \times 100\%$$

Apoptosis assay

HUVEC cells were plated in 60-mm dishes at 2×10^5 cells per dish and allowed to attach overnight. The cells were then treated with rAAV-IgG-endostatin at a dose of 1×10^6 vp, rAAV-MCS at a dose of 1×10^6 vp as positive control and RPMI 1640 as negative control. The cells were harvested 72 h after infection, washed twice with PBS. (a) First, the cells were stained by Hoechst 33258 to analyse apoptosis. (b) Next, these cells were resuspended in 100 μl of binding buffer provided in the Annexin V-FITC/PI apoptosis detection kit and then 5 μl Annexin V-FITC and 5 μl PI solution were added; the cells were gently centrifuged and incubated for 15 min at room temperature in the dark. Finally, 400 μl of binding buffer was added to each tube and this was followed by flow cytometry.

Animal experiment

Balb/c nude mice aged 4–5 weeks were obtained from Vital River Laboratory (Beijing, China) and maintained under specific pathogen-free conditions, with food and water supplied ad libitum. All animal experiments were approved by the committee on the use and care of animals of Guanzhou Medical University. To establish xenografts, animals were inoculated intramuscularly in the left hind leg with 2×10^6 T24 tumour cells suspended in 200 μl of 0.9% saline. When tumour volume reached about 200 mm^3, mice were randomly assigned to three groups (n=5 mice per group) and were administered rAAV-IgG-endostatin, rAAV-MCS at a dose of 1×10^{11} vp or RPMI 1640 via intra-tumoural injection every second day for a maximum of six times. Tumour growth was observed for 30 days by measuring the tumour size every 3 days using calipers. Tumour volume (V) was calculated by using the formula: tumour volume

$$V\left(\text{mm}^3\right) = \pi/6 \times \text{Length(mm)} \times \text{Width(mm)}^2.$$

At the end of the experiment, tumours were harvested for additional analyses as described further. Differences in the rate of tumour growth were tested for statistical significance. Tumours and tissues were removed for subsequent analysis after sacrificing the animals. The heart, liver, spleen, kidney and lung were collected for detection of the viral spread and pathological change.

Immunohistochemistry of CD34 and vascular assessment

Tumour micro-vessels were stained using a monoclonal antibody to the CD34 antigen on endothelial cells. Entire tumour sections were reconstructed using tiled field mapping and the total tumour areas as well as the tumour necrosis was determined using an image-analysis program. Estimates of tumour angiogenesis were made on the sections attained with CD34 using the Chalkley counting method on vessel hotspots. The vessels were counted at

high magnification (×200) and the number of points on CD34 highlighted micro-vessels was recorded. The Chalkey count for an individual tumour was taken as the mean of the random fields. All animals in these studies were pre-coded and tumour sections were counted in a blinded manner.

Statistical analysis

All data are reported as mean±standard deviation(SD) values. Student's *t*-test was applied to study the relationship between the difference variables. The significance level was defined as $p<0.05$.

Results

Construction of pAAV-IgG-endostatin

Endostatin DNA was amplified from pAAV-IgG-endostatin using PCR. A fragment measuring about 700 bp, which is consistent with the required size, was amplified. The transgene expression cassette is flanked by the non-coding ITRs, which are the only wild-type viral sequences present in this recombinant vector genome and are essential for packaging of the viral vector DNA. The ITR sequence was also amplified using only one primer (5′-AGGAACCCCTAGTGATGGAG); the fragment measured about 3 kb (sequence size between two ITRs of pAAV-IgG-endostatin), which indicated a stable sequence.

Generation of rAAV viral particles

The packaging and purification of recombination AAV were generated as described previously, and the titres of rAAV were presented as virus particles. We isolated, concentrated and purified rAAV by a three-step procedure, as described previously. The procedure was performed within 4 h. More than 100-folds of concentration could be achieved from the initial material. The recovery of rAAV infectious from the initial material was estimated to be more than 90%.

The capsid of AAV-2 is composed of three kinds of proteins: VP1, VP2 and VP3, with molecular weight of 87, 72 and 62 ku, respectively. The ratio of VP1, VP2 and VP3 in AAV-2 viron is 1:1:10. Therefore, three bands with specific patterns could be seen when the virons were analysed by SDS-PAGE. In our experiment, the purity of rAAV was analysed by Coomassie brilliant blue-stained SDS acrylamide gel electrophoresis. Three clear bands representing the AAV capsid proteins VP1,VP2 and VP3 could be seen on both lanes against a very low background, which demonstrated that chloroform extraction could effectively extract contaminants from rAAV stock without significant loss of the rAAV (Fig. 2a). The purity of rAAV was estimated to be more than 95% in the final stock by our computer analysis. An aliquot of the purified rAAV stock after negative staining was taken to visualise virus particles by electron microscopy scan. Large amounts of rAAV particles with clean background could be seen clearly. Most of the AAV particles appear full with few intermediate particles (Fig. 2b). The result indicates that the purified rAAV stock contains virus particles of high concentration and purity.

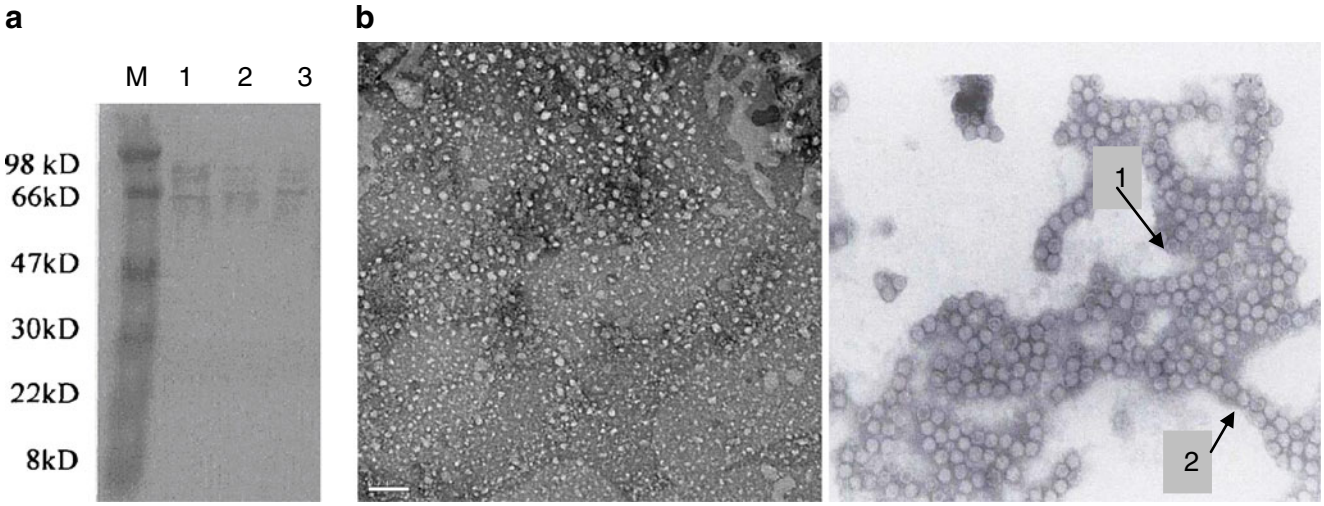

Fig. 2 **a** Coomassie brilliant blue stained SDS-polyacrylamide gel electrophoresis of rAAV at various stages of purification. Each stock was mixed with an equal volume of two loading buffers and incubated in boiling water for 3 min before loading. A 10-μl sample was loaded in each lane. The purified rAAV is shown in lanes 1–3. M, standard proteins whose molecular weights are indicated on the *left*. **b** Purified and concentrated rAAV particles visualized by electron microscopy after negative staining with uranyl acetate (bar = 0.2 μm). *Arrow 1* indicates intermediate virus and *arrow 2* full virus

Cell stability after rAAV transduction

rAAV genome-containing particles were determined by the AVSachTM ELISA kit. The physical titre of purified rAAV is estimated to be about 2×10^{11} vp. To prove the cell-targeting ability and stability after transduction of rAAV, we first detected specific EGFP expression in T24 cell lines at a gradient titre of 10^3, 10^4, 10^5, 10^6 and 2×10^6 vp. As shown in Fig. 3, after infection about 72 h, the green fluorescent were observed under fluorescence microscopy. At the same time, the expression of EGFP gene was time dependent and reached maximal levels 72 h after infection. We further analysed the titre value by flow cytometry to determine the appropriate value to be applied in later study and the ratios of the EGFP expression were 2%, 5%, 35%, 62% and 57% at different doses of 10^3, 10^4, 10^5, 10^6 and 2×10^6 vp, respectively. Therefore, we considered rAAV 1×10^6 vp as the appropriate titre value and applied it in the later stages of the study.

To further explore the cell stability after rAAV transduction, we then investigated the T24 cells cycle about 72 h after infection of rAAV-IgG-endostatin by FACS (Table 1). Genomic DNA were also extracted from the cells infected with rAAV-IgG-endostatin. The DNA sequence of endostatin was identified as measuring about 700 bp by PCR and sequence analysis and this was consistent with the endostatin sequence. These results suggested that the bladder tumour cells were stable after being infected by rAAV.

rAAV-IgG-endostatin specifically suppressed endothelial cell proliferation and induced apoptosis

First, we tested the effect of rAAV-IgG-endostatin on cell viability using rAAV-EGFP particles as a positive control. Two cell lines, HUVEC and AAV-293, were infected with rAAV-IgG-endostatin, rAAV-EGFP particles or RPMI 1640, and cell viability over time was analysed by the MTT assay. As shown in Fig. 4a, the cell viability in HUVEC line transduced with rAAV-IgG-endostatin decreased to approximately 50–60% in a time-dependent manner. No significant changes in the viability of AAV-293 cells were observed up to 72 h after transduction. The cytotoxic effect of rAAV-IgG-endostatin in HUVEC cell was more apparent than that of rAAV-EGFP. Based on MTTs, rAAV-IgG-endostatin was found to induce suppression of cell proliferation or increase in cell death in HUVEC cells. We then investigated whether it could selectively induce apoptosis in HUVEC cells again. First, as shown in Fig. 4b, apoptosis analysis by using annexin V staining indicated that the concentration of apoptotic HUVEC cells after transduction with rAAV-IgG-endostatin was 35.6± 1.99%, compared with only 8.35±1.28% and 5.32±1.82% by rAAV-EGFP and RPMI 1640, respectively. Furthermore, examination of apoptotic morphological changes in cells was performed by Hoechst 33258 staining. HUVEC cells treated by rAAV-IgG-endostatin showed obvious apoptosis (Fig. 4c), while apoptosis was not observed in HUVEC cells tranduced with rAAV-EGFP and RPMI 1640. rAAV-IgG-endostatin was finally found to induce a significant increase in apoptosis in HUVEC cells. Together, these results confirmed that the inhibition of endothelial cells mediated by rAAV-IgG-endostatin was associated with the apoptotic process.

Antitumour activity of rAAV-IgG-endostatin on bladder cancer xenograft in vivo

To test whether recombinant endostatin production by rAAV-mediated gene transfer could have a direct inhibitory effect on tumour cell-induced angiogenesis

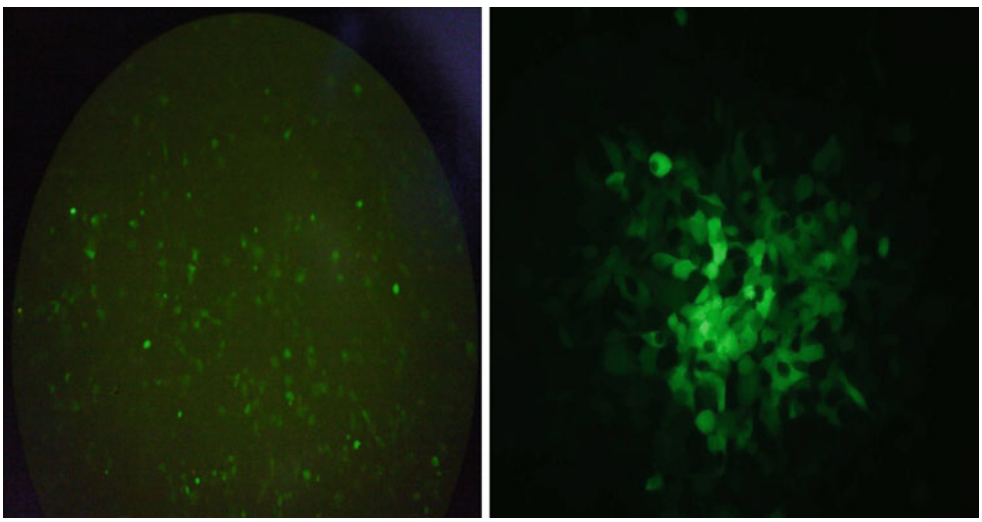

(×100) (×400)

Fig. 3 Tumour-specific EGFP expression. Tumour cell line T24 was infected with rAAV-EGFP at a titer of 1×10^6 vp. The green fluorescent cells were observed under fluorescence microscopy after 72 h

Table 1 Cell cycle analysis of T24 cells

	Ratio of cell cycle (%)		
Cells	G1	S	G2
T24	50.5	41.2	8.3
T24 (infected)	52.4	40.5	7.1

*$p>0.05$, no significant difference between T24 cells and infected T24 cells, that is, rAAV had no influence on tumor cell cycle distribution

in vivo, various doses of rAAV-IgG-endostatin were injected intramuscularly into nude mice, and serum endostatin levels were determined (Fig. 5). Results showed that dose-dependent plateauing of serum endostatin levels was reached 5–7 weeks after injection. This expression profile is likely a consequence of the known delay in the onset of the expression of the transgene by rAAV vectors, a phenomenon believed to be due to the vector DNA's gradual conversion into double-stranded forms by leading-strand synthesis prior to establishing stable expression.

A 1×10^{11}-vp dose of rAAV-IgG-endostatin resulted in a serum endostatin level (~400 ng/ml; Fig. 5) that was sufficient to inhibit tumour cell-induced angiogenesis in vivo. This is clearly evident in Fig. 6, which illustrates that T24 cells injected into nude mice possessing elevated serum endostatin levels after rAAV-IgG-endostatin injections induced significantly fewer blood vessels than tumour cells in control mice or mice injected with the rAAV-MCS vector.

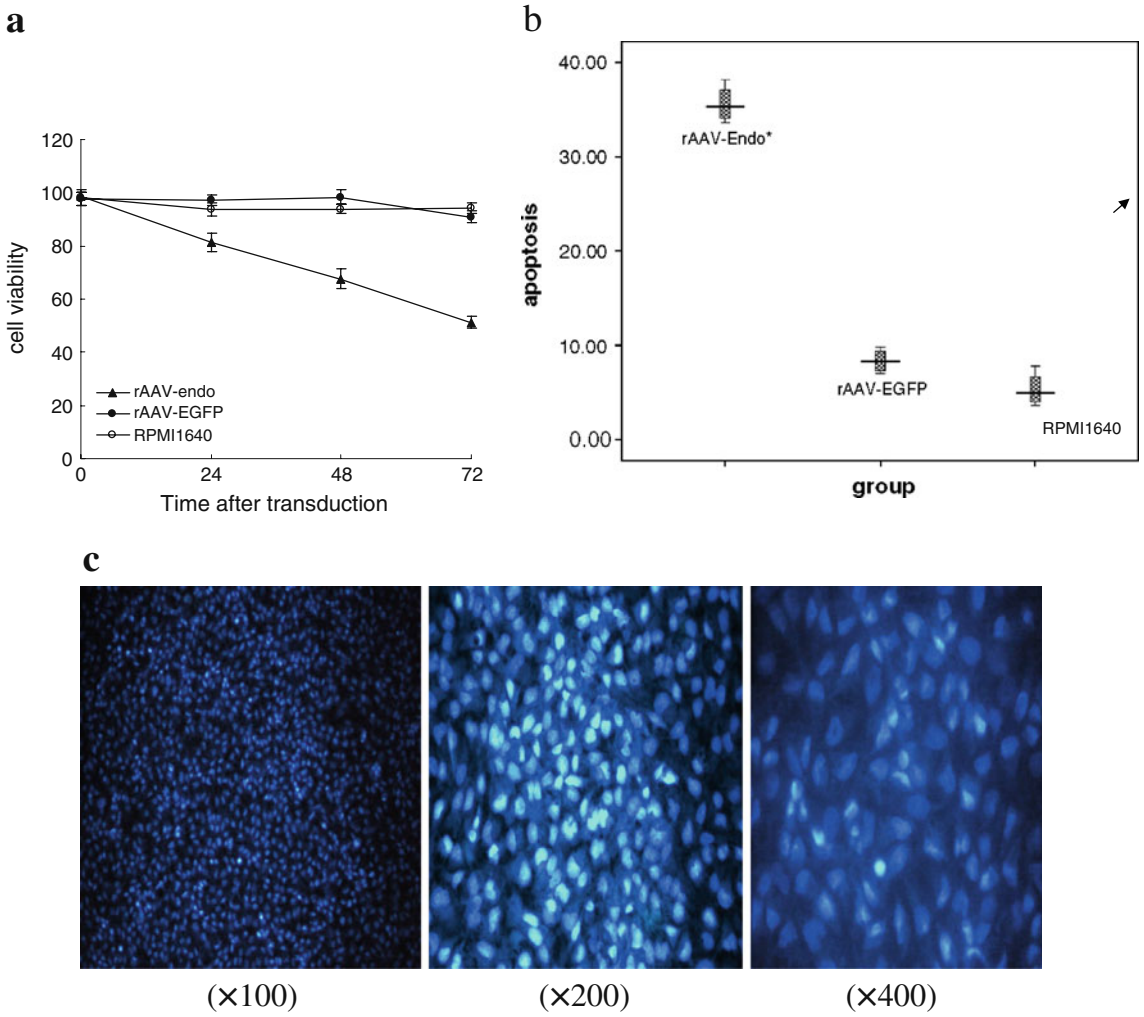

Fig. 4 **a** Cell viability was measured by MTT assay in the HUVEC cell line and AAV-293 cell at 24–72 h after infection, rAAV-IgG-endostatin, rAAV-EGFP and RPMI1640. **b**–**c** Detection of endothelial cell apoptosis induced by rAAV-IgG-endostatin. **b** Percentage of apoptosis was measured by annexin V staining. First, HUVEC cells were harvested after infection with rAAV-IgG-Endostatin at a titer of 1×10^{6} vp for 72 h, then these infected cells were stained with annexin V-FITC; flow cytometry was immediately performed for apoptosis assay. The percentage of apoptotic cell was calculated with CellQuest software. Each value represents the mean of three wells; *$p<0.05$. **c** Hoechst 33258 staining assay. Cells were treated in the same manner as described in panel b, and apoptotic changes of HUVEC cells were analyzed by Hoechst 33258 staining. *Arrows* refer to apoptosis cells

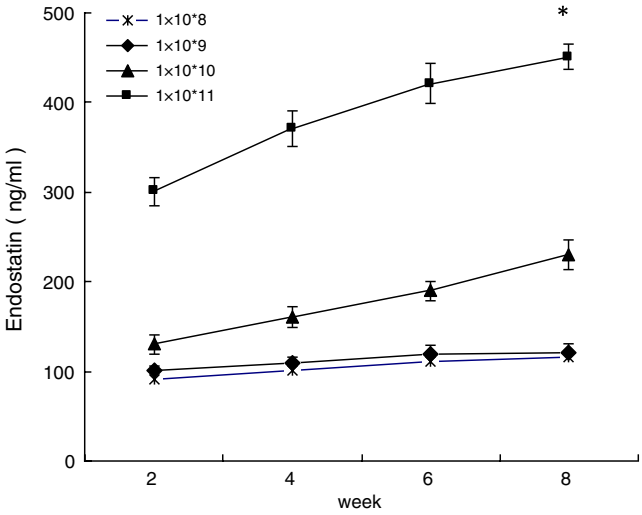

Fig. 5 Serum endostatin levels in nude mice as a function of time after intramuscular injections of various doses of rAAV-IgG-endostatin. Endostatin levels were determined by ELISA kit. Each datum point represents the mean±standard deviation (SD) of the animals. *Asterisk* indicates statistically significant difference ($p<0.05$) from untreated control animals

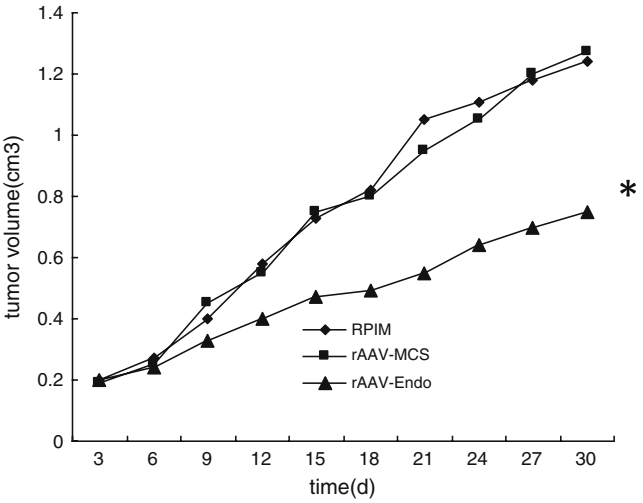

Fig. 7 Effect of rAAV gene transfer of rAAV-MCS or endostatin on the growth of bladder cancer T24 xenografts. The growth of the median tumour in each group is shown. The times for the tumours in mice treated with rAAV-IgG-Endostatin were significantly different from those of the untreated control group ($p<0.05$)

The results showed that the tumours in mice injected with the rAAV-IgG-endostatin not only took significantly longer to emerge but also that their growth, once established, was significant slower than that of tumours grown in untreated or rAAV-MCS-treated animals (Fig. 7). To quantify these differences, the time to grow from a fixed size (200 mm^3) to one that was five times larger (1,000 mm^3) was evaluated (Fig. 8). Although all mice in various treatment groups eventually developed tumours, tumours growing in rAAV-IgG-endostatin-treated animals took significantly longer to reach the size of ~1,000 mm^3. The subsequent growth rates of establishing tumours (time to grow from 200 to 1,000 mm^3) were also significantly delayed in rAAV-IgG-endostatin-treated hosts. These data suggested that rAAV-IgG-endostatin suppresses tumour formation and growth in the animals.

We finally investigated the potential toxicity induced by rAAV infection in major organs, including the heart, liver, spleen, kidneys and lungs, by HE. We detected no pathological change among these tissues that demonstrated rAAV expression.

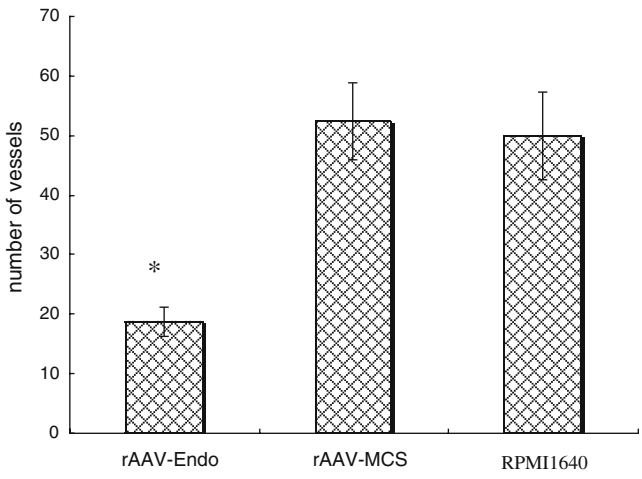

Fig. 6 Effect of elevated serum levels of endostatin on the number of vessels induced by T24 tumour cells. The number of vessels was counted using a dissecting microscope. Data were evaluated by a Wilcoxon rank-sum test and were presented as the median, 25–75% and 10–90% values per group. *Asterisk* indicates a statistically significant difference ($p<0.05$) from untreated control animals

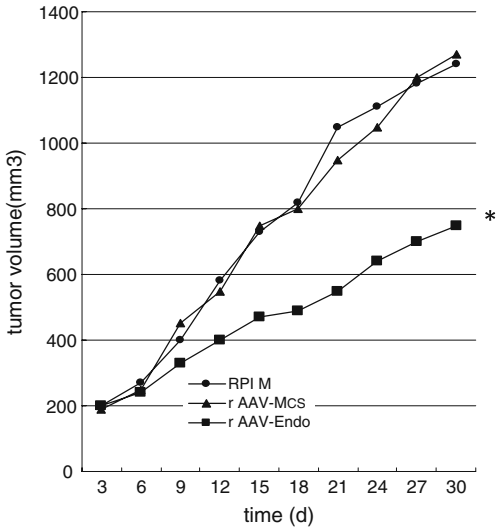

Fig. 8 Time for T24 tumours to growth to five times their starting size. Mice were either untreated or treated with rAAV-IgG-Endostatin or rAAV-MCS at the doses indicated. They indicated a statistically significant difference ($p<0.05$) from untreated control animals

Discussion

To date, most endostatin investigations have utilised the purified protein form [20–22]. While large-scale production of recombinant endostatin appears feasible, difficulties associated with providing large quantities of this agent for chronic treatment as well as strategies to maintain therapeutic serum levels of endostatin over a prolonged course of treatment remain. The delivery of endostatin through a gene-encoding strategy provides a potentially attractive alternative by offering the possibility of enduring benefits from a single or limited numbers of treatments. Although initial attempts at non-viral delivery of endostatin through the direct injection of naked DNA or systemic administration of plasmids resulted in some anti-tumour effects in mice, such approaches could only achieve transient low levels of circulating endostatin [23–25]. The use of microencapsulated stable endostatin cells offered an intriguing alternative [26], but this strategy is unlikely to translate into application in the clinical setting. Perhaps the most promising approach lies in the use of virus-based delivery systems. Indeed, high circulating endostatin levels, sufficient to inhibit tumour growth in mice, have been attained with adenoviral vector constructs [27–29]. However, this application is limited by its toxicity and immunogenicity [8].

Gene therapy represents an attractive approach to treat cancers and other chronic diseases, and the development of an effective delivery system is absolutely critical to the usefulness and safety of gene therapy. Safety, efficiency and a consistent delivery system are major issues of concern for gene therapy in targeting tumour tissues [8]. At present, the AAV vector has the most promising potential, due to its non-pathogenicity, wide tropisms and long-term transgenic expression in vivo [30]. Our laboratory has been exploring the alternative possibility of utilising AAV-mediated gene transfer of endostatin as an anti-angiogenic therapeutic strategy. Such vectors have been used to successfully introduce, with high efficiency and long-term stability, foreign genes into many types of fully mature, differentiated cells both in vitro and in vivo [31]. The delivery of anti-angiogenic agents such as endostatin may be well suited for such an approach. Previous work by Nguyen and colleagues [32, 33] demonstrated an inhibitory effect of rAAV-delivered endostatin on endothelial cell growth in vitro. However, there are only a few reports on the application of rAAVs in bladder cancer. In the present investigation, we expanded these studies to evaluate the efficacy of rAAV-mediated expression of endostatin in vivo and, in particular, to examine whether elevated serum endostatin levels has an effect on bladder tumours.

In our study, endostatin cDNA was inserted into an rAAV plasmid and the resulting rAAV was designated rAAV-IgG-endostatin. Inhibition of endothelial cell growth by endostatin has been previously documented. This was confirmed in the present studies using HUVEC endothelial cells. Our results showed that 3-day treatment with recombinant endostatin at 60 ng/ml inhibited HUVEC proliferation by 50–60% ($p<0.05$). Of note is the finding that conditioned media derived from cultures of a stable clone of 293 cells infected with the rAAV-EGFP control vector affected neither endothelial cell proliferation nor migration. The biological activities of recombinant endostatin by AAV gene transfer were further confirmed by its effect on endothelial cell apoptosis and cell-cycle distribution. We then investigated whether it could selectively induce apoptosis in HUVEC cells again. First, as shown in Fig. 4b, apoptosis analysis by using annexin V staining indicated that concentrations of apoptotic HUVEC cells after transduction with rAAV-IgG-endostatin was 36.6%, compared with only 8.35% and5.32% by rAAV-EGFP and RPMI 1640, respectively. Furthermore, evaluation of cellular apoptotic morphological changes by Hoechst 33258 staining was performed. HUVEC cells treated by rAAV-IgG-endostatin showed obvious apoptosis. In contrast, endostatin treatment had no effect on T24 bladder tumour cell apoptosis or cell-cycle distribution. Our results confirmed that the inhibition of endothelial cells mediated by rAAV-IgG-endostatin was associated with the apoptosis process.

We have observed that with AAV-delivered human endostatin the intramuscular injection of rAAV-IgG-endostatin led to rAAV dose-dependent increases in serum endostatin levels by 4 weeks, which plateauing of these levels by 5–7 weeks. These levels were subsequently maintained until the experiments were terminated. Our experience suggested that the highest vector doses of endostatin led to significant delays in tumour appearance and growth. In addition, the present study further showed that this effect was vector dose-dependent such that even a moderate but well-sustained elevation of endostatin was sufficient to inhibit the initiation and growth of T24 xenografts. These data support the notion that endogenous endostatin levels may play an important role in the regulation of tumour-induced angiogenesis and growth.

In conclusion, we demonstrated an effective system for bladder gene therapy with a two-part safeguard, that is, an ideal vector and an efficient gene. We showed that a gene therapy approach using an AAV-mediated gene-transfer strategy to deliver endostatin can significantly suppress tumour-induced angiogenesis and also enhance the treatment of tumour growth. The data suggest that this approach deserves further consideration as an adjuvant in the treatment of bladder carcinoma with conventional anti-cancer therapies and provides a potentially useful and safer strategy for cancer gene therapy.

Acknowledgements This work was supported by the Medical Scientific Research Foundation of Guangdong Province, China (no. A2010255).

Conflicts of interest None declared

References

1. Malkowicz SB. Intravesical therapy for superficial bladder cancer. Semin Urol Oncol. 2000;18:280–8.
2. Edelman MJ. New approaches to treatment of metastatic bladder cancer. Curr Oncol Rep. 2000;2:379–85.
3. Block T. Chemotherapy of bladder carcinoma. Current status and trends. Urologe A. 1994;33:557–67.
4. Witjes JA, Wullink M, Oosterhof GO, de Mulder P. Toxicity and results of MVAC (methotrexate, vinblastine, adriamycin and cisplatin) chemotherapy in advanced urothelial carcinoma. Eur Urol. 1997;31:414–9.
5. Freund CTF, Tong XW, Rowley D, Engehausen D, Frolov A, Kieback DG, et al. Combination of adenovirus-mediated thymidine kinase gene therapy with cytotoxic chemotherapy in bladder cancer in vitro. Urol Oncol Semin Orig Invest. 2003;21:197–205.
6. Folkman J. Angiogenesis in cancer, vascular, rheumatoid and other disease. Nat Med. 1995;1:27–31.
7. Persano L, Crescenzi M, Indraccolo S. Anti-angiogenic gene therapy of cancer: current status and future prospects. Mol Aspects Med. 2007;28:87–114.
8. Shi W, Teschendorf C, Muzyczka N, Siemann DW. Gene therapy delivery of Endostatin enhances the treatment efficacy of radiation. Radiother Oncol. 2003;66:1–9.
9. Yu YF, Chen ZW, Li ZM, Li ZH, Lu S. The effects of cetuximab alone and in combination with endostatin on vascular endothelial growth factor and interleukin-8 expression in human lung adenocarcinoma cells. Curr Ther Res. 2009;70:116–28.
10. Zhang Y, Ma H, Zhang J, Liu S, Liu Y, Zheng D. AAV-mediated TRAIL gene expression driven by hTERT promoter suppressed human hepatocellular carcinoma growth in mice. Life Sci. 2008;82:1154–61.
11. Ponnazhagan S, Mahendra G, Kumar S, Shaw DR, Stockard CR, Grizzle WE, et al. Adeno-associated virus 2-mediated antiangiogenic cancer genetherapy: long-term efficacy of a vector encoding encoding angiostatin and endostatin over vectors encoding a single factor. Cancer Res. 2004;64:781–7.
12. Ma H, Liu Y, Liu S, Kung HF, Sun X, Zheng D, et al. Recombinant adeno-associated virus-mediated TRAIL gene therapy suppresses liver metastatic tumors. Int J Cancer. 2005;116:314–21.
13. Shi J, Zheng D, Liu Y, Sham MH, Tam P, Farzaneh F, et al. Overexpression of soluble TRAIL induces apoptosis in human lung adenocarcinoma and inhibits growth of tumor xenografts in nude mice. Cancer Res. 2005;65:1687–92.
14. Subramanian IV, Ghebre R, Ramakrishnan R. Adeno-associated virus mediated delivery of a mutant Endostatin suppresses ovarian carcinoma growth in mice. Gene Ther. 2005;12:30–8.
15. Streck CJ, Dickson PV, Ng CY, Zhou J, Gray JT, Nathwani AC, et al. Adeno-associated virus vector-mediated systemic delivery of IFN-beta combined with low-dose cyclophosphamide affects tumor regression in murine neuroblastoma models. Clin Cancer Res. 2005;11:6020–9.
16. Samulski RJ, Zhu X, Xiao X, Brook JD, Housman DE, Epstein N, et al. Targeted integration of adeno-associated virus (AAV) into human chromosome 19. EMBO J. 1991;10:3941–50.
17. El-Aneed A. An overview of current delivery systems in cancer gene therapy. J Control Release. 2004;94:1–14.
18. AAV Helper-Free System Instruction Manual. Revision A.02. www.stratagene.com
19. Wu X, Dong X, Wu Z, Cao H, Niu D, Qu J, et al. A novel method for purification of recombinant adeno-associated virus vectors on a large scale. Chin Sci Bull. 2001;6:485–90.
20. Bertolini F, Fusetti L, Mancuso P, Gobbi A, Corsini C, Ferrucci PF, et al. Endostatin, an antiangiogenic drug, induces tumor stabilization after chemotherapy or anti-CD20 therapy in a NOD/SCID mouse model of human high-grade non-Hodgkin lymphoma. Blood. 2000;96:282–7.
21. Bloch W, Huggel K, Sasaki T, Grose R, Bugnon P, Addicks K, et al. The angiogenesis inhibitor Endostatin impairs blood vessel maturation during wound healing. Fed Am Soc Exp Biol J. 2000;14:2373–6.
22. Dhanabal M, Ramchandran R, Volk R, Stillman IE, Lombardo M, Iruela-Arispe ML, et al. Endostatin: yeast production, mutants, and antitumor effect in renal cell carcinoma. Cancer Res. 1999;59:189–97.
23. Blezinger P, Wang J, Gondo M, Quezada A, Mehrens D, French M, et al. Systemic inhibition of tumor growth and tumor metastases by intramuscular administration of the Endostatin gene. Nat Biotechnol. 1999;17:343–8.
24. Chen QR, Kumar D, Stass SA, Mixson AJ. Liposomes complexed to plasmids encoding angiostatin and Endostatin inhibit breast cancer in nude mice. Cancer Res. 1999;59:3308–12.
25. Szary J, Szala S. Intra-tumoral administration of naked plasmid DNA encoding mouse Endostatin inhibits renal carcinoma growth. Int J Cancer. 2001;91:835–9.
26. Joki T, Machluf M, Atala A, Zhu J, Seyfried NT, Dunn IF, et al. Continuous release of Endostatin from microencapsulated engineered cells for tumor therapy. Nat Biotechnol. 2001;19:35–9.
27. Chen CT, Lin J, Li Q, Phipps SS, Jakubczak JL, Stewart DA, et al. Antiangiogenic gene therapy for cancer via systemic administration of adenoviral vectors expressing secretable Endostatin. Hum Gene Ther. 2000;11:1983–96.
28. Feldman AL, Restifo NP, Alexander HR, Bartlett DL, Hwu P, Seth P, et al. Antiangiogenic gene therapy of cancer utilizing a recombinant adenovirus to elevate systemic Endostatin levels in mice. Cancer Res. 2000;60:1503–6.
29. Sauter BV, Martinet O, Zhang WJ, Mandeli J, Woo SL. Adenovirus mediated gene transfer of Endostatin in vivo results in high level of transgene expression and inhibition of tumor growth and metastases. Proc Natl Acad Sci USA. 2000;97:4802–7.
30. Wu Z, Asokan A, Samulski RJ. Adeno-associated virus serotypes: vector tool kit for human gene therapy. Mol Ther. 2006;14:316–27.
31. Xiao X, Li J, Samulski RJ. Efficient long-term gene transfer into muscle tissue of immunocompetent mice by adeno-associate virus vector. J Virol. 2009;70:8098–108.
32. Nguyen JT. Adeno-associated virus and other potential vectors for angiostatin and Endostatin gene therapy. Adv Exp Med Biol. 2000;465:457–66.
33. Nguyen JT, Wu P, Clouse ME, Hlatky L, Terwilliger EF. Adeno-associated virus-mediated delivery of antiangiogenic factors as an antitumor strategy. Cancer Res. 2008;58:5673–7.